Published in final edited form as:
Biochemistry. 2010 August 3; 49(30): 6358–6364. doi:10.1021/bi100773g.

Mechanistic Investigation of the Inhibition of Aβ42 Assembly and Neurotoxicity by Aβ42 C-terminal Fragments

Huiyuan Li[1], **Bernhard H. Monien**[1,8], **Aleksey Lomakin**[5], **Reeve Zemel**[1], **Erica A. Fradinger**[1,9], **Miao Tan**[2], **Sean M. Spring**[1], **Brigita Urbanc**[7], **Cui-Wei Xie**[2,3], **George B. Benedek**[5,6], and **Gal Bitan**[1,3,4,*]

[1]Department of Neurology, David Geffen School of Medicine

[2]Department of Psychiatry and Biobehavioral Sciences, David Geffen School of Medicine

[3]Brain Research Institute, University of California at Los Angeles, CA

[4]Molecular Biology Institute, University of California at Los Angeles, CA

[5]Materials Processing Center, Massachusetts Institute of Technology, Cambridge, MA

[6]Department of Physics, Massachusetts Institute of Technology, Cambridge, MA

[7]Physics Department, Drexel University, Philadelphia, PA

Abstract

Oligomeric forms of amyloid β-protein (Aβ) are key neurotoxins in Alzheimer's disease (AD). Previously, we found that C-terminal fragments (CTFs) of Aβ42 interfered with assembly of full-length Aβ42 and inhibited Aβ42-induced toxicity. To decipher the mechanism(s) by which CTFs affect Aβ42 assembly and neurotoxicity, here, we investigated the interaction between Aβ42 and CTFs using photo-induced cross-linking and dynamic light scattering. The results demonstrate that distinct parameters control CTF inhibition of Aβ42 assembly and Aβ42-induced toxicity. Inhibition of Aβ42-induced toxicity was found to correlate with stabilization of oligomers with hydrodynamic radius (R_H) = 8–12 nm and attenuation of formation of oligomers with R_H = 20–60 nm. In contrast, inhibition of Aβ42 paranucleus formation correlated with CTF solubility and the degree to which CTFs formed amyloid fibrils themselves but did not correlate with inhibition of Aβ42-induced toxicity. Our findings provide an important insight into the mechanisms by which different CTFs inhibit the toxic effect of Aβ42 and suggest that stabilization of non-toxic Aβ42 oligomers is a promising strategy for designing inhibitors of Aβ42 neurotoxicity.

Keywords

Amyloid β-protein; aggregation; neurotoxicity; inhibitor; dynamic light scattering

Alzheimer's Disease (AD) is the most common neurodegenerative disease, affecting over 35 million people worldwide (1). Abundant evidence suggests that oligomeric forms of amyloid

*To whom correspondence should be addressed: Department of Neurology, David Geffen School of Medicine, University of California at Los Angeles, Neuroscience Research Building 1, Room 451, 635 Charles E. Young Drive South, Los Angeles, CA 90095-7334, USA. gbitan@mednet.ucla.edu. Tel.: +1-310-206-2082; Fax.: +1-310-206-1700..
[8]Current address: Deutsches Institut für Ernährungsforschung Potsdam-Rehbrücke, Abt. Ernährungstoxikologie, Arthur-Scheunert-Allee 114-116, 14558 Nuthetal, Germany.
[9]Current address: Department of Biology, Whittier College, 13406 E Philadelphia St., Whittier, CA 90608

SUPPORTING INFORMATION AVAILABLE Figures S1–S3 presenting examples of PICUP–SDS-PAGE analysis, Aβ(30–40) inhibitory assays, and correlation analysis are available free of charge via the Internet at http://pubs.acs.org.

β-protein (Aβ) are the main neurotoxins causing AD (2,3). Two main forms of Aβ exist *in vivo*, containing 40 (Aβ40) or 42 (Aβ42) amino acid residues. Aβ42 plays a central role in the pathogenesis of AD (4,5). Compared to Aβ40, Aβ42 is substantially more toxic, forms higher-order oligomers, and follows a different oligomerization pathway (6,7). Peptide inhibitors of Aβ assembly and neurotoxicity reported previously mainly targeted Aβ fibril formation (8). The sequences of such inhibitors were based on random selection (9), self-recognition of the central hydrophobic cluster (CHC) of Aβ (10–13), or structural modifications of sequences from the CHC or C-terminal regions (14–17). As the hypothesis of the cause of AD shifted from Aβ fibril formation and deposition to oligomeric Aβ, the design strategy for peptide inhibitors for treatment of AD was adjusted to target Aβ oligomerization. In view of the important role of the C-terminus in Aβ42 assembly and toxicity, we hypothesized that the C-terminal fragments (CTFs) of Aβ42 might disrupt Aβ42 assembly and inhibit its neurotoxicity. In a previous study, we confirmed this hypothesis and found that Aβ42 CTFs, [Aβ(x–42), x = 28–39], with the exception of Aβ(28–42), inhibited Aβ42-induced neurotoxicity (18). Among these CTFs, Aβ(31–42) and Aβ(39–42) displayed outstanding inhibitory effects. In addition to inhibiting Aβ42-induced neuronal death, these CTFs were found to rescue disruption of synaptic activity by Aβ42 oligomers at micromolar concentrations (18). Initial biophysical assessment suggested that these two CTFs exerted their inhibitory activity via distinct mechanisms (18). However, to gain further mechanistic understanding, additional investigation of the characteristics of the CTFs themselves, and of their interaction with Aβ42, including comparison of Aβ(31–42) and Aβ(39–42) to other CTFs with low or high activity, was necessary.

Recently, we reported a systematic characterization of biophysical properties of all the CTFs in the original series (19), to which we added for additional structural insight two Aβ40 CTFs, Aβ(34–40) and Aβ(30–40), and a fragment derived from the putative folding nucleus of Aβ, Aβ(21–30) (20). We found that most of Aβ42 CTFs longer than 8 residues readily formed β-sheet-rich fibrils, whereas the shorter CTFs did not. The two Aβ40 CTFs were substantially less prone to aggregation than their Aβ42 CTF counterparts (19). Surprisingly, Aβ(30–40) was found to be a strong inhibitor of Aβ42-induced toxicity. Importantly, we found that the capability of the CTFs to inhibit Aβ42 toxicity did not correlate with their propensity to aggregate or form β-sheet-rich amyloid structures. Rather, inhibition of toxicity appeared to correlate with a coil-turn structure identified by molecular dynamics simulations using experimental ion-mobility spectrometry/mass-spectrometry data as structural constraints (21).

To better understand the mechanism(s) by which CTFs inhibit Aβ42-induced toxicity, we asked whether they inhibited Aβ42 assembly, and if so, to what extent inhibition of Aβ42 assembly correlated with inhibition of Aβ42-induced toxicity. Here we used photo-induced cross-linking of unmodified proteins (PICUP) and dynamic light scattering (DLS) to study Aβ42 assembly in the absence or presence of CTFs and control peptides and correlated the findings with our previously-published data on inhibition of Aβ42 toxicity. The sequences of all the peptides used are shown in Table 1.

MATERIALS AND METHODS

Peptide preparation

Aβ42, CTFs and control peptides were synthesized by solid-phase techniques (22), using 9-fluorenylmethoxycarbonyl (FMOC) chemistry, as described previously (19,23,24), purified by high-performance liquid chromatography and analyzed by mass spectrometry and amino acid analysis (AAA).

Cell viability assays

Previously, a cell-viability screen showed that all Aβ42 CTFs, except Aβ(28–42), which was highly toxic itself, inhibited Aβ42-induced toxicity (18). Under similar conditions, Aβ(30–40) showed strong inhibitory activity, whereas Aβ(34–40) and Aβ(21–30) were inactive (19). Here we used dose-dependent lactate dehydrogenase (LDH) experiments to evaluate the inhibition of Aβ(30–40) dose-dependently. The method was described previously (18). Briefly, Aβ42:Aβ(30–40) mixtures of concentration ratios 1:0, 1:1, 1:2, 1:5, 1:10 were added to the differentiated rat pheochromocytoma (PC-12) cells and incubated for 48 h. Cell death was assessed by the CytoTox-ONE Homogenous Membrane Integrity Assay (LDH assay; Promega, Madison, WI). Three independent experiments with six replicates (n = 18) were carried out, and the results were averaged and presented as mean ± SEM.

Electrophysiological studies

Spontaneous miniature excitatory postsynaptic currents (mEPSCs) of mouse primary hippocampal neurons in the presence of Aβ42 and in the absence or presence of Aβ(31–42) or Aβ(39–42) were reported previously (18). Here we used the same method to measure Aβ42 in the presence of Aβ(30–40). Briefly, cells were perfused at a flow rate of 0.4–0.5 mL/min with peptide samples of 3 μM Aβ42 and Aβ42:Aβ(30–40) at 1:10 concentration ratio, or vehicle control (extracellular solution with equal volume of DMSO to that used to dissolve the peptide). To calculate mEPSC amplitude and frequency, events were analyzed for 1 min before, and every 5 min during the application of peptide samples. mEPSC frequency data are presented as mean ± SEM.

Photo-induced cross-linking of unmodified proteins (PICUP)

PICUP experiments for Aβ(31–42) and Aβ(39–42) were described previously (18). Here we expanded these experiments to the entire series of Aβ42 CTFs, the two Aβ40 CTFs, and Aβ(21–30). Briefly, peptides were dissolved in 60 mM NaOH and diluted with 10 mM sodium phosphate, pH 7.4. Low molecular weight (LMW) Aβ42 was prepared by filtration through a 10-kDa molecular weight cut-off filter (MWCO) (25) or by centrifugation at 16,000 *g* for 10 min (because some batches of Aβ42 had low solubility and yielded insufficient concentration for PICUP experiments). Solutions of Aβ fragments were sonicated for 1 min and then filtered through an Anotop 10 syringe filter with 20-nm pore size (Whatman, Florham Park, NJ). The final concentration of each peptide was determined by AAA. The solution of LMW Aβ42 was mixed with different nominal concentrations of Aβ fragments and the mixtures were cross-linked immediately, fractionated by SDS-PAGE, silver stained, and subjected to densitometric analysis using ONE-Dscan (Scanalytics, Fairfax, VA). Three replicates were measured for each peptide. The abundance of Aβ42 hexamer was normalized to the entire lane, and reported as mean ± SEM. IC_{50} values were calculated by fitting of hexamer abundance vs. logarithm of CTF concentration using Prism (GraphPad, La Jolla, CA)

Dynamic light scattering (DLS)

Solutions of Aβ42 in the absence or presence of CTFs were measured using an in-house-built optical system with a He-Ne laser (wavelength 633 nm, power 50 mW; Coherent, Santa Clara, CA) as a light source and using either PD2000DLS or multitau PD4047 Precision Detectors correlators. The size distribution of scattering particles was reconstructed from the scattered light correlation function using PrecisionDeconvolve software (Precision Detectors, Bellingham, MA) based on the regularization method by Tikhonov and Arsenin (26).

Peptides were prepared in UCLA by dissolution in 60 mM NaOH and diluted with 10 mM sodium phosphate (pH 7.4). Aβ42:CTF mixtures contained 30 μM each of Aβ42 and Aβ(x–42), with x = 29, 30, 31, 32, 35 or 39, or Aβ(30–40). For transportation from UCLA to MIT for measurements, two hundred μL samples were lyophilized stored at −20°C, and shipped. The samples then were reconstituted in 200 μL water. The solutions were sonicated for 1 min and filtered through an Anotop 10 syringe filter (20-nm pore size) prior to DLS measurements. The hydrodynamic radius and intensity of particles were recorded. The particle growth rate (dR_H/dt), i.e., the increase of hydrodynamic radius over time, was determined using at least 20 measurements of 10 min each taken immediately after sample preparation and no less than 10 measurements taken on the next day. The data are presented as mean ± SEM. Three replicates were measured for each peptide.

RESULTS

Aβ42 oligomerization in the presence of CTFs

Previously, using PICUP (27) the oligomer size distribution of Aβ42 was found to contain abundant pentamers and hexamers, which were termed “paranuclei” (6). The abundance of these paranuclei, particularly the hexamers, was found to be a sensitive probe for testing inhibition of Aβ42 oligomerization (28). Importantly, because all Aβ fragments used here contained only residues that have low reactivity in PICUP chemistry (18,28), cross-linking of CTFs to Aβ42 or to themselves was not observed, facilitating unhindered analysis of Aβ42 oligomer size distributions. LMW Aβ42 was prepared by filtration through a 10-kDa MWCO filter (25) at ~30 M, mixed with increasing concentrations of each peptide, and cross-linked. The cross-linked mixtures were analyzed by SDS-PAGE and densitometry. Examples are shown in Supplementary Figure S1.

Previously, we found that Aβ(31–42) inhibited Aβ42 hexamer formation dose-dependently, whereas Aβ(39–42) did not (18). Here, all other Aβ42 CTFs, Aβ40 CTFs, and Aβ(21–30) were tested. Analysis of densitometric data showed that Aβ(36–42) and shorter Aβ42 CTFs at concentrations above 100 μM did not inhibit Aβ42 hexamer formation (Figure S1C). Similarly, Aβ40 CTFs and Aβ(21–30) had no effect on Aβ42 hexamer formation (Figure 1). In contrast, Aβ(35–42) and longer Aβ42 CTFs caused a dose-dependent decrease of Aβ42 hexamer abundance (Figures 1, S1A and S1B). The inhibitory activity increased with peptide length from Aβ(35–42) through Aβ(33–42), whereas additional elongation to Aβ(32–42) and Aβ(31–42) had little effect on activity. Remarkably, further elongation to Aβ(30–42) and Aβ(29–42) resulted in ~2 orders of magnitude increase in inhibitory activity, yielding nanomolar IC_{50} values.

Aβ42 particle growth in the presence of CTFs

To further evaluate the interaction between CTFs and Aβ42, we used DLS. PICUP and DLS are complementary methods for investigation of Aβ assembly. PICUP offers high-resolution detection of low-order oligomers, whereas DLS enables non-invasive detection of high-order assemblies with high sensitivity (6,29). Out of the twelve Aβ42 CTFs, we selected six for DLS characterization of their interactions with full-length Aβ42. Aβ(30–42), Aβ(31–42), and Aβ(39–42) were studied because they were the strongest inhibitors of Aβ42-induced neurotoxicity (18). Aβ(29–42) was included as the most potent inhibitor of Aβ42 hexamer formation (Figure 1). Aβ(32–42) was selected because it stood out in the CTF series. This CTF was slightly toxic itself, was less efficient than Aβ(31–42) or Aβ(33–42) as an inhibitor of Aβ42-induced toxicity, and displayed unusual aggregation behavior, namely forming predominantly amorphous, rather than fibrillar, aggregates (19). Aβ(35–42) was selected as a negative control with relatively low inhibitory activity in both the toxicity (18) and the

oligomerization (Figure 1) assays. Finally, Aβ(30–40) was studied as a potent (IC_{50} = 29 ± 4 μM in the LDH assay) Aβ40-derived inhibitor of Aβ42-induced neurotoxicity (Figure S2).

Similar to previous observations (6), in the absence of CTFs, immediately after preparation, Aβ42 comprised predominantly two populations of particles. Particles with hydrodynamic radius R_{H1} = 8–12 nm, which remained largely unchanged during the measurements, and particles with R_{H2} = 20–60 nm, which were observed in some measurements and tended to fluctuate substantially. We name these oligomer populations *P*1 and *P*2, respectively. Note that the large oligomers comprising the *P*2 fraction cannot possibly pass through a 20-nm pore size filter and therefore must form immediately after filtration. After several days, large particles, presumably fibrils, formed (Figure 2, bottom panel). The long CTFs themselves, e.g., Aβ(29–42), Aβ(30–42), Aβ(31–42), and Aβ(30–40) showed aggregation in DLS measurements (19). However, because in the equimolar mixtures of CTF and Aβ42 used here the CTF mass is several times lower than that of Aβ42, the contribution of CTF to the observed scattering is negligible.

In the presence of the seven CTFs we tested, immediately after preparation, a significant enrichment of population *P*2 was observed (Figure 2, first column). It is important to consider, however, that the scattering intensity is proportional to the square of the average mass of particles in each fraction. Thus, although the relative contribution of *P*2 particles to the observed scattering was large, their weight fraction in the Aβ42:CTF mixtures was still no more than a few percent. During the experiments, the size of *P*1 remained relatively unchanged, whereas *P*2 appeared to grow in size. Notably, substantial differences in *P*2 growth rate, dR_{H2}/dt, were observed in the presence of different CTFs (Figure 3A). In fact, the strongest toxicity inhibitor, Aβ(31–42), decreased dR_{H2}/dt substantially by 60±13% relative to Aβ42 alone. Aβ(39–42), had a weaker effect on dR_{H2}/dt decreasing the rate by 35±28%. Other CTFs had little or no effect.

Interestingly, on day 1, smaller R_H values were observed in the presence of Aβ(39–42) (R_{H1} = 6 ± 3 nm, R_{H2} = 30 ± 10 nm) relative to other CTFs. Similarly, in the presence of Aβ(30–40) *P*1 particles had R_{H1} = 6 ± 3 nm on day 1, though *P*2 particles were larger than in the presence of other CTFs. Because both peptides were among the strongest inhibitors of Aβ42-induced toxicity, these data suggested a correlation between inhibition of toxicity and smaller size of oligomers corresponding to *P*1 particles.

The relative abundance of *P*1 and *P*2 particles showed substantial differences among mixtures of Aβ42 with different CTFs. *P*2 particles appeared to be less abundant in the presence of the CTFs that had been found to be effective inhibitors of toxicity (18). For example, in the presence of Aβ(30–40), *P*2 particles contributed 20% of the scattering on day 2 and 4% on day 7. In contrast, in the presence of Aβ(29–42), which showed weak inhibition of Aβ42-induced toxicity, *P*2 particles contributed 74% of the scattering on day 2 and 87% on day 7. Notably, in the presence of Aβ(29–42), the scattering intensity, but not the particle size, grew ~5-times as fast as in all other samples (data not shown), suggesting that aggregates of similar size had larger mass, i.e., were more dense compared to aggregates of Aβ42 alone or in the presence of other CTFs.

In addition to measuring particle size, we also measured the frequency of intensity spikes that occur when large particles cross the laser beam (Figure 3B). This measurement is a convenient proxy of formation of very large particles, presumably fibrils, before they become so large that they precipitate out of solution. Aβ(29–42), Aβ(30–42), Aβ(31–42), and Aβ(30–40) showed inhibition of fibril growth relative to Aβ42 in the absence of CTFs or in the presence of the shorter CTFs, Aβ(32–42), Aβ(35–42), and Aβ(39–42).

DISCUSSION

Inhibition of Aβ assembly is an attractive pathway to developing reagents that will block Aβ toxicity and potentially will lead to treatment for AD. Because the assembly process of Aβ is complex and the relationship between assembly size and structure and toxicity are not well understood, it is important to understand the mechanisms by which inhibitors affect Aβ assembly and how the resulting structures correlate with inhibition of toxicity. Such structure–activity analysis may lead eventually to the ability to predict factors necessary for successful inhibition of Aβ toxicity.

Here, we used two complementary methods, PICUP and DLS, for studying the interaction of peptide inhibitors with Aβ42, and compared the data with our previous characterization of inhibition of Aβ42-induced toxicity by these peptides (18) and the biophysical features of the peptides themselves (19). The PICUP data showed that Aβ(35–42) and longer CTFs interrupted Aβ42 paranucleus formation, whereas the shorter peptides did not. The order of activity of the CTFs in inhibiting hexamer formation in this assay roughly followed CTF length and did not explain the relatively high potency with which Aβ(30–42), Aβ(31–42), Aβ(39–42), or Aβ(30–40) inhibited Aβ42-induced toxicity.

DLS measurements showed that CTFs interacted with Aβ42 and stabilized two oligomer populations. The data suggested several lines of correlation between inhibition of Aβ42-induced toxicity and the assembly behavior of different CTFs. The two previously-characterized toxicity inhibitors, Aβ(31–42) and Aβ(39–42) showed the strongest reduction of growth rate of *P*2 particles, dR_{H2}/dt. However, slow growth rate alone did not explain the behavior of other CTFs, such as Aβ(30–42) or Aβ(30–40), which showed strong inhibition of Aβ42-induced toxicity but had little effect on dR_{H2}/dt. A decrease in the size of *P*1 particles was observed in the presence of Aβ(39–42) or Aβ(30–40), but not other CTFs. Inhibition of formation of putative fibrils measured by the effect of CTFs on the frequency of intensity spikes correlated only partially with inhibition of toxicity and did not provide satisfactory mechanistic explanation for the toxicity results. These analyses suggested that more than one mechanism might be responsible for inhibition of Aβ42-induced toxicity by CTFs.

To gain additional mechanistic insight, we examined potential sets of correlation among the different data sets, including inhibition of paranucleus formation (Figure 1), abundance of *P*2 particles (Figure 2), inhibition of toxicity ((18) and Figure S2A), CTF solubility (19), CTF conversion to β-sheet-rich fibrils (19), and CTF particle growth (19). We calculated linear correlations among these data sets, which, depending on the parameter and the availability of the data, ranged from 4–7 data points. The analysis confirmed a poor correlation between inhibition of paranucleus formation and inhibition of Aβ42-induced neurotoxicity ($r^2 = 0.01$, Figure 4A). Inhibition of paranucleus formation showed relatively high correlation with CTFs solubility ($r^2 = 0.72$, Figure 4B), β-sheet formation ($r^2 = 0.96$, Figure S3A), and particle size increase ($r^2 = 0.94$, Figure S3B). The error bars of the solubility and particle growth rate of the CTFs alone in Figure 4 and Figure S3 are inherently quite large due to the large variability in amyloid peptide samples (30). These errors are reflected in the calculated r^2 and p values for the linear correlations. The correlation calculated might raise a concern regarding precipitation of Aβ42 in the presence of the least soluble CTFs. However, neither SDS-PAGE analysis of cross-linked oligomers (Figure S1) nor the DLS measurements (Figure 2) showed such precipitation or reduced solubility. Thus, our analysis suggests that the same forces that reduce aqueous solubility and promote fibrillogenesis of CTFs in the absence of Aβ42 also facilitate the interaction of the CTFs with Aβ42 leading to inhibition of paranucleus formation.

Out of the different parameters we measured in the DLS experiments (dR_{H2}/dt, the abundance of *P*2 particles, and intensity), we found that inhibition of Aβ42-induced toxicity correlated with a low abundance of *P*2 particles on day 2 ($r^2 = 0.90$, Figure 4C) and on day 4–7 ($r^2 = 0.75$, data not shown). Thus, although the particle distribution initially had increased contribution of *P*2 particles in the presence of all CTFs relative to Aβ42 alone, on subsequent days, the relative contribution of *P*2 particles was small for strong inhibitors of toxicity and large for weak inhibitors. For reasons that are not entirely clear, Aβ(30–42) was an outlier and therefore was not included in this analysis.

Though the DLS experiments were done under conditions that differ from those of toxicity experiments, the high correlation between low abundance of *P*2 and Aβ42-induced toxicity at 48 h provides important insights into the mechanism(s) by which CTFs might inhibit the toxicity. This putative mechanism is summarized in Figure 5. In the absence of CTFs (Figure 5, top path), Aβ monomers rapidly self-assemble into small oligomers (*P*1 particles). Association of these oligomers into larger assemblies (*P*2 particles) is relatively slow, whereas the conversion of *P*2 assemblies into fibrils or their disassembly back into *P*1 oligomers is fast. As a result, little accumulation of *P*2 particles is observed. In the presence of CTFs (Figure 5, bottom path), Aβ42 and the CTFs co-assemble into heterooligomers. the size of which is generally similar to that of the oligomers formed in the absence of CTFs. The CTFs stabilize both *P*1 and *P*2 oligomers and retard the conversion of *P*2 assemblies into fibrils. However CTFs vary in their effect on the conversion of the small *P*1 oligomers into the larger *P*2 oligomers. Effective inhibitors slow down this process and give rise to predominantly *P*1 oligomers, whereas less effective inhibitors allow for a relatively fast *P*1→*P*2 conversion. Thus, the anti-correlation between *P*2 abundance and inhibition of toxicity suggest that a predominant mechanism by which CTFs inhibit Aβ42 toxicity is by stabilizing *P*1 heterooligomers.

Taken together, our data indicate that CTFs affect Aβ42 assembly in different ways, including disruption of paranucleus formation by Aβ(35–42) and longer Aβ42 CTFs, stabilization of *P*1 and *P*2 particles by all CTFs, alteration of the size and abundance of *P*1 and *P*2 assemblies, and co-assembly with Aβ42 into heterooligomers. Inhibition of Aβ42 toxicity by CTFs correlates with accumulation of *P*1 heterooligomers suggesting attenuation of *P*1→*P*2 conversion. Stabilization of non-toxic Aβ oligomers is a mechanism shared by other inhibitors of Aβ assembly and toxicity, including *scyllo*-inositol (31) and (−)-epigallocatechin gallate (32). Thus, we propose that efforts geared towards designing inhibitors of protein self-assembly should focus on diversion of the process towards formation of non-toxic oligomers (or heterooligomers of Aβ and the inhibitor) that can be degraded by cellular clearance mechanisms rather than attempting to prevent monomer self-association.

Supplementary Material

Refer to Web version on PubMed Central for supplementary material.

Acknowledgments

The work was supported by grants AG027818 from NIH/NIA and 2005/2E from the Larry L. Hillblom Foundation.

Abbreviations

AAA	amino acid analysis
Aβ	amyloid β-protein

AD	Alzheimer's disease
CHC	central hydrophobic cluster
CTF	C-terminal fragment
DLS	dynamic light scattering
LDH	lactate dehydrogenase
LMW	low molecular weight
mEPSC	miniature excitatory postsynaptic currents
MWCO	molecular weight cut-off filter
PICUP	photo-induced cross-linking of unmodified proteins

REFERENCES

1. Prince, M.; Jackson, J., editors. Alzheimer's Disease International World Alzheimer Report 2009. Alzheimer's Disease International; London: 2009.
2. Hardy J, Selkoe DJ. The amyloid hypothesis of Alzheimer's disease: progress and problems on the road to therapeutics. Science. 2002; 297:353–356. [PubMed: 12130773]
3. Ferreira ST, Vieira MN, De Felice FG. Soluble protein oligomers as emerging toxins in Alzheimer's and other amyloid diseases. IUBMB Life. 2007; 59:332–345. [PubMed: 17505973]
4. Dahlgren KN, Manelli AM, Stine WB Jr. Baker LK, Krafft GA, LaDu MJ. Oligomeric and fibrillar species of amyloid-β peptides differentially affect neuronal viability. J. Biol. Chem. 2002; 277:32046–32053. [PubMed: 12058030]
5. Roher AE, Lowenson JD, Clarke S, Woods AS, Cotter RJ, Gowing E, Ball MJ. β-Amyloid-(1–42) is a major component of cerebrovascular amyloid deposits: implications for the pathology of Alzheimer disease. Proc. Natl. Acad. Sci. USA. 1993; 90:10836–10840. [PubMed: 8248178]
6. Bitan G, Kirkitadze MD, Lomakin A, Vollers SS, Benedek GB, Teplow DB. Amyloid β-protein (Aβ) assembly: Aβ40 and Aβ42 oligomerize through distinct pathways. Proc. Natl. Acad. Sci. USA. 2003; 100:330–335. [PubMed: 12506200]
7. Chen Y-R, Glabe CG. Distinct early folding and aggregation properties of Alzheimer amyloid-β peptides Aβ40 and Aβ42: stable trimer or tetramer formation by Aβ42. J. Biol. Chem. 2006; 281:24414–24422. [PubMed: 16809342]
8. Sciarretta KL, Gordon DJ, Meredith SC. Peptide-based inhibitors of amyloid assembly. Methods Enzymol. 2006; 413:273–312. [PubMed: 17046402]
9. Hughes SR, Goyal S, Sun JE, Gonzalez-DeWhitt P, Fortes MA, Riedel NG, Sahasrabudhe SR. Two-hybrid system as a model to study the interaction of β-amyloid peptide monomers. Proc. Natl. Acad. Sci. USA. 1996; 93:2065–2070. [PubMed: 8700886]
10. Tjernberg LO, Naslund J, Lindqvist F, Johansson J, Karlstrom AR, Thyberg J, Terenius L, Nordstedt C. Arrest of β-amyloid fibril formation by a pentapeptide ligand. J. Biol. Chem. 1996; 271:8545–8548. [PubMed: 8621479]
11. Soto C, Kindy MS, Baumann M, Frangione B. Inhibition of Alzheimer's amyloidosis by peptides that prevent β-sheet conformation. Biochem. Biophys. Res. Commun. 1996; 226:672–680. [PubMed: 8831674]
12. Lowe TL, Strzelec A, Kiessling LL, Murphy RM. Structure-function relationships for inhibitors of β-amyloid toxicity containing the recognition sequence KLVFF. Biochemistry. 2001; 40:7882–7889. [PubMed: 11425316]
13. Pallitto MM, Ghanta J, Heinzelman P, Kiessling LL, Murphy RM. Recognition sequence design for peptidyl modulators of β-amyloid aggregation and toxicity. Biochemistry. 1999; 38:3570–3578. [PubMed: 10090743]

14. Adessi C, Frossard MJ, Boissard C, Fraga S, Bieler S, Ruckle T, Vilbois F, Robinson SM, Mutter M, Banks WA, Soto C. Pharmacological profiles of peptide drug candidates for the treatment of Alzheimer's disease. J. Biol. Chem. 2003; 278:13905–13911. [PubMed: 12578830]
15. Hughes E, Burke RM, Doig AJ. Inhibition of toxicity in the β-amyloid peptide fragment β -(25–35) using N-methylated derivatives: a general strategy to prevent amyloid formation. J. Biol. Chem. 2000; 275:25109–25115. [PubMed: 10825171]
16. Gordon DJ, Tappe R, Meredith SC. Design and characterization of a membrane permeable N-methyl amino acid-containing peptide that inhibits Aβ1–40 fibrillogenesis. J. Pept. Res. 2002; 60:37–55. [PubMed: 12081625]
17. Pratim Bose P, Chatterjee U, Nerelius C, Govender T, Norstrom T, Gogoll A, Sandegren A, Gothelid E, Johansson J, Arvidsson PI. Poly-N-methylated amyloid β-peptide (Aβ) C-terminal fragments reduce Aβ toxicity in vitro and in Drosophila melanogaster. J. Med. Chem. 2009; 52:8002–8009. [PubMed: 19908889]
18. Fradinger EA, Monien BH, Urbanc B, Lomakin A, Tan M, Li H, Spring SM, Condron MM, Cruz L, Xie CW, Benedek GB, Bitan G. C-terminal peptides coassemble into Aβ42 oligomers and protect neurons against Aβ42-induced neurotoxicity. Proc. Natl. Acad. Sci. USA. 2008; 105:14175–14180. [PubMed: 18779585]
19. Li H, Monien BH, Fradinger EA, Urbanc B, Bitan G. Biophysical characterization of Aβ42 C-terminal fragments: inhibitors of Aβ42 neurotoxicity. Biochemistry. 2010; 49:1259–1267. [PubMed: 20050679]
20. Lazo ND, Grant MA, Condron MC, Rigby AC, Teplow DB. On the nucleation of amyloid β-protein monomer folding. Protein Sci. 2005; 14:1581–1596. [PubMed: 15930005]
21. Wu C, Murray MM, Bernstein SL, Condron MM, Bitan G, Shea JE, Bowers MT. The structure of Aβ42 C-terminal fragments probed by a combined experimental and theoretical study. J. Mol. Biol. 2009; 387:492–501. [PubMed: 19356595]
22. Merrifield RB. Automated synthesis of peptides. Science. 1965; 150:178–185. [PubMed: 5319951]
23. Lomakin A, Chung DS, Benedek GB, Kirschner DA, Teplow DB. On the nucleation and growth of amyloid β-protein fibrils: Detection of nuclei and quantitation of rate constants. Proc. Natl. Acad. Sci. USA. 1996; 93:1125–1129. [PubMed: 8577726]
24. Condron MM, Monien BH, Bitan G. Synthesis and purification of highly hydrophobic peptides derived from the C-terminus of amyloid β-protein. Open Biotechnol. J. 2008; 2:87–93. [PubMed: 19898686]
25. Bitan G, Teplow DB. Preparation of aggregate-free, low molecular weight amyloid-β for assembly and toxicity assays. Methods Mol. Biol. 2005; 299:3–9. [PubMed: 15980591]
26. Tikhonov, AN.; Arsenin, VY. Solution of III-Posed Problems. Halsted Press; Washington, DC: 1977.
27. Fancy DA, Kodadek T. Chemistry for the analysis of protein-protein interactions: rapid and efficient cross-linking triggered by long wavelength light. Proc. Natl. Acad. Sci. USA. 1999; 96:6020–6024. [PubMed: 10339534]
28. Bitan G. Structural study of metastable amyloidogenic protein oligomers by photo-induced cross-linking of unmodified proteins. Methods Enzymol. 2006; 413:217–236. [PubMed: 17046399]
29. Teplow DB, Lazo ND, Bitan G, Bernstein S, Wyttenbach T, Bowers MT, Baumketner A, Shea JE, Urbanc B, Cruz L, Borreguero J, Stanley HE. Elucidating amyloid β-protein folding and assembly: A multidisciplinary approach. Acc. Chem. Res. 2006; 39:635–645. [PubMed: 16981680]
30. May PC, Gitter BD, Waters DC, Simmons LK, Becker GW, Small JS, Robison PM. β-Amyloid peptide in vitro toxicity: lot-to-lot variability. Neurobiol. Aging. 1992; 13:605–607. [PubMed: 1281290]
31. McLaurin J, Golomb R, Jurewicz A, Antel JP, Fraser PE. Inositol stereoisomers stabilize an oligomeric aggregate of Alzheimer amyloid β peptide and inhibit Aβ -induced toxicity. J. Biol. Chem. 2000; 275:18495–18502. [PubMed: 10764800]
32. Ehrnhoefer DE, Bieschke J, Boeddrich A, Herbst M, Masino L, Lurz R, Engemann S, Pastore A, Wanker EE. EGCG redirects amyloidogenic polypeptides into unstructured, off-pathway oligomers. Nat. Struct. Mol. Biol. 2008; 15:558–566. [PubMed: 18511942]

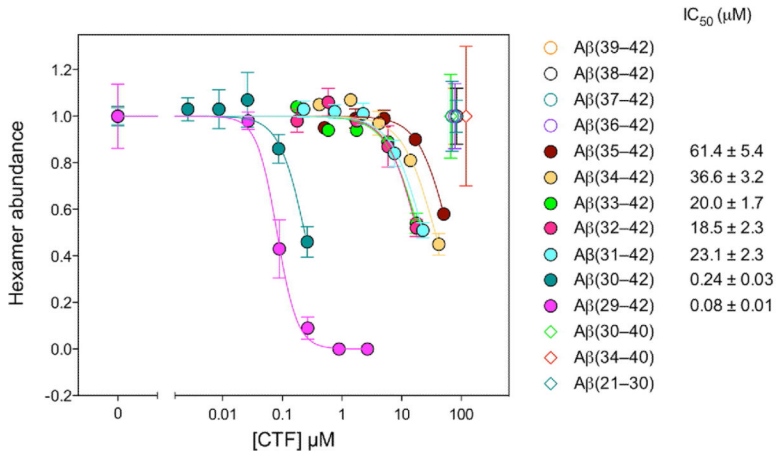

Figure 1.

Inhibition of Aβ42 hexamer formation. Aβ42 was cross-linked in the absence or presence of increasing concentrations of each CTF and analyzed by SDS-PAGE and silver staining. The amount of Aβ42 hexamer was determined densitometrically and normalized to the protein content in the entire lane. IC_{50} values are the CTF concentration required for 50% inhibition of Aβ42 hexamer formation.

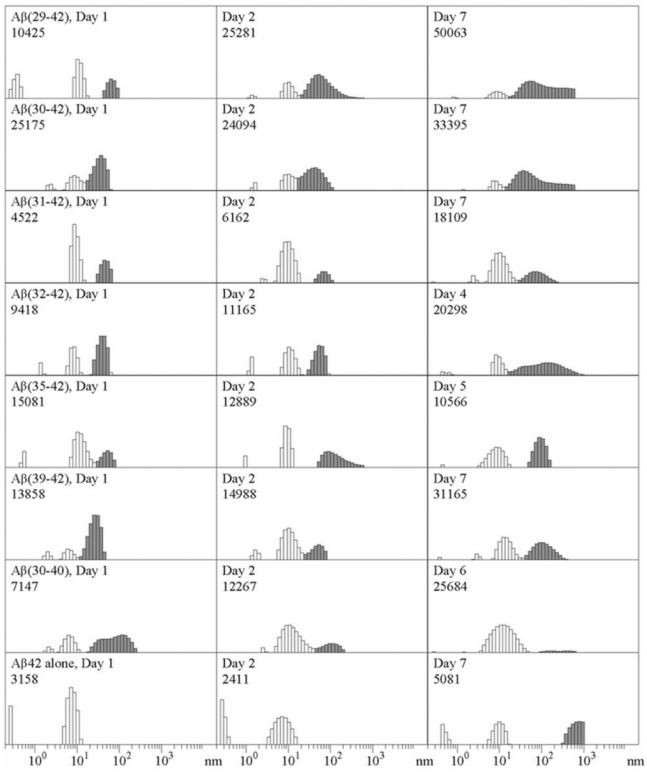

Figure 2.

CTF effect on Aβ42 particle size distribution. Representative distributions of Aβ42 in the absence or presence of CTFs immediately after preparation (*Left*), on the next day (*Center*), and after 4–7 days (*Right*). White bars represent *P*1 particles. Gray bars represent *P*2 or larger particles (in the case of Aβ42 alone). Days of measurement and the total scattering intensities in counts per second are shown in the upper left corner of each panel. Only intensities within the same row are directly comparable with each other.

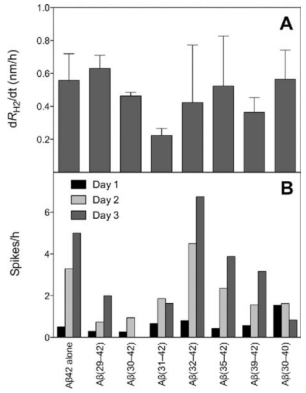

Figure 3.

DLS monitoring of Aβ42 aggregation in the absence or presence of CTFs. A) Growth rates (dR_{H2}/dt) of particles with initial R_{H2} = 20–60 nm. The data for Aβ42 alone could not be obtained consistently (see text). B) Intensity spikes per hour indicating fibril development.

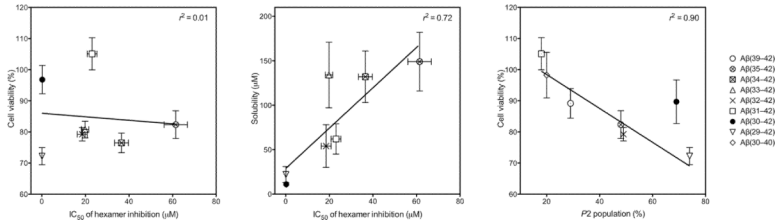

Figure 4.

Correlation analysis. A) Linear regression analysis correlating inhibition of paranucleus formation for Aβ(29–42)–Aβ(35–42) with inhibition of Aβ42-induced toxicity (19) (r^2 = 0.01, p = 0.8). B) Linear regression analysis correlating inhibition of paranucleus formation for Aβ(29–42)–Aβ(35–42) with CTFs solubility (19) (r^2 = 0.72, p = 0.02). C) Linear regression analysis correlating the population of *P*2 on day 2 for Aβ(29–42)–Aβ(32–42), Aβ(35–42), Aβ(39–42), and Aβ(30–40) with inhibition of Aβ42-induced toxicity (r^2 = 0.90, p = 0.004). Aβ(30–40) is an outlier in this correlation, which is not included in the calculation.

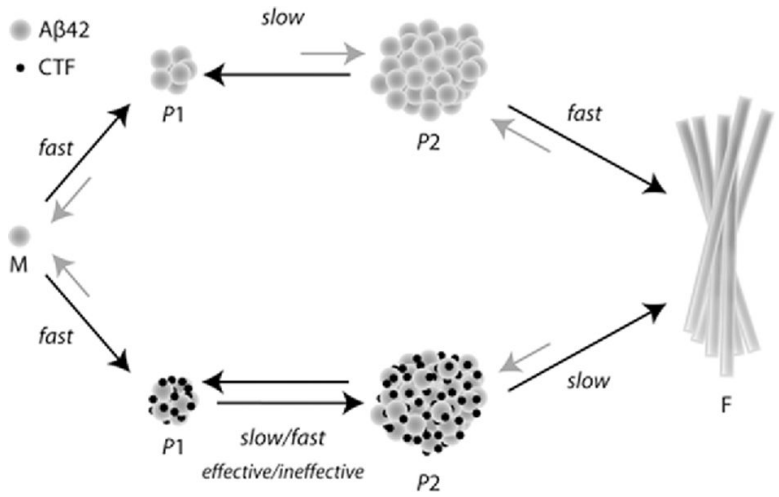

Figure 5.

Schematic representation of a putative mechanism by which CTFs affect Aβ42 assembly. Monomer (M) assembly into *P*1 particles is a fast process in the absence (top path) or presence (bottom path) of CTFs. CTFs may accelerate the conversion of *P*1 into *P*2 oligomers, but effective inhibitors of Aβ42-induced toxicity induce slower acceleration than ineffective ones, shifting the population towards *P*1. All CTFs slow down the maturation of *P*2 assemblies into fibrils (F).

Table 1

Peptide code and sequence.

Peptide	Sequence
Aβ(39–42)	VVIA
Aβ(38–42)	GVVIA
Aβ(37–42)	GGVVIA
Aβ(36–42)	VGGVVIA
Aβ(35–42)	MVGGVVIA
Aβ(34–42)	LMVGGVVIA
Aβ(33–42)	GLMVGGVVIA
Aβ(32–42)	IGLMVGGVVIA
Aβ(31–42)	IIGLMVGGVVIA
Aβ(30–42)	AIIGLMVGGVVIA
Aβ(29–42)	GAIIGLMVGGVVIA
Aβ(28–42)	KGAIIGLMVGGVVIA
Aβ(34–40)	LMVGGVV
Aβ(30–40)	AIIGLMVGGVV
Aβ(21–30)	AEDVGSNKGA